**Proceedings of the ASME 2026 Smart Materials
Adaptive Structures and Intelligent Systems
SMASIS2026
September 13–16, 2026, Albuquerque, NM, USA**

SMASIS2026-191393

FPGA-DEPLOYABLE APPROXIMATE TOPOLOGICAL FRAMEWORK FOR LOW-LATENCY CHANGE-POINT DETECTION IN PCB SHOCK AND VIBRATION RESPONSE

Mohsen Gol Zardian[1], Charlton Rolle[2], Trotter Roberts[1], Joud N. Satme[1], Arman Razmarashooli[3], Austin R. J. Downey[1,*], Jason D. Bakos[2], Simon Laflamme[3], Gurcan Comert[4], and Negash Begashaw[5]

[1]Mechanical Engineering, University of South Carolina, Columbia, SC, USA
[2]Computer Science and Engineering, University of South Carolina, Columbia, SC, USA
[3]Department of Civil, Construction and Environmental Engineering, Iowa State University, Iowa, USA
[4]Department of Computational Data Science and Engineering, North Carolina State University, Greensboro, NC, USA
[5]School of Science and Engineering, Benedict College, Columbia, SC, USA

ABSTRACT

Shock detection in electronic and printed circuit board (PCB) assemblies is critical for real-time control methods, as abrupt impacts drive high transient accelerations that trigger solder joint damage, component cracking, decontamination, and intermittent electrical faults. Identifying the shock onset with minimal delay enables active control systems to respond before damage propagates. This work introduces a change-point detection approach based on approximate Topological Data Analysis (TDA) features, termed Feature Assessment Segmented Temporally with Topological Data Analysis (FAST-TDA), extracted from streaming sensor measurements. Fast-TDA retains the most informative topological signature of a delay-embedded signal while removing the main computational bottleneck of conventional TDA by replacing persistence diagram computation with direct geometric surrogates on the embedded point cloud. These features remain stable during steady vibration and change sharply at shock onset. In this work, the ellipse-fitting stage of Fast-TDA is implemented as a hardware-optimized pipeline on an FPGA using a cyclic Jacobi solver, enabling deterministic low-latency operation at high sampling rates. A sequential change-point The test is applied to the resulting feature stream to localize shock onset with minimal delay.

Keywords: high-rate dynamic systems, shock detection, Fast Topological data analysis (TDA), ellipse fitting

1. INTRODUCTION

High-rate dynamic systems undergo rapid and extreme changes within extremely short timeframes, typically less than 100 ms, with accelerations often surpassing 100 g_n [1]. Such systems appear in diverse applications ranging from hypersonic vehicles and active blast mitigation devices to ballistic packages and electronic assemblies [2]. Abrupt shock events in PCB assemblies can induce transient accelerations that degrade solder-joint reliability and cause component-level failures [3], while board-level drop-test studies have shown that such dynamic loading can degrade solder-joint reliability [4]. Early shock-onset detection is essential for initiating protective responses before damage propagation occurs [5].

High-rate structural health monitoring and prognostics provide the broader context for this work, emphasizing the need for rapid sensing, feature extraction, and decision-making in systems subjected to short-duration dynamic events [1]. Active vibration mitigation has also been investigated for electronic assemblies, where active mass damping has been shown to reduce vibration levels in electronic circuit boards [6]. More recent studies have extended active vibration control concepts to smart structures subjected to internal mechanical shock, highlighting the importance of rapid response under impulsive loading conditions [7]. In addition, finite element modeling of fixed-fixed beams under shock excitation with active control has provided a useful computational framework for studying transient structural response and control strategies in configurations related to the experimental platform used in this work [8].

Topological Data Analysis (TDA) has emerged as a powerful data-driven alternative capable of extracting shape-based features directly from time-series signals [2]. TDA has been used to characterize complex nonlinear behavior in dynamical systems, including chaos detection [9]. It has also been introduced as a useful framework for extracting structural-dynamic features in structural health monitoring applications [10]. In the full TDA approach, the acceleration signal is first embedded into a high-dimensional point cloud via Takens' delay embedding. Persistent homology is then computed to generate persistence diagrams,

*Corresponding author: austindowney@sc.edu

from which scalar topological descriptors such as the maximum persistence of H_1, Wasserstein amplitudes, and Betti numbers are extracted and supplied to a downstream regressor [2]. This pipeline effectively captures the underlying attractor geometry of the system, yet it requires the construction of persistence diagrams at every time window [2].

In Feature Assessment Segmented Temporally with Topological Data Analysis (FAST-TDA), the acceleration signal is first reconstructed into a low-dimensional point cloud using Takens' delay embedding, which creates delay vectors from the original time series to approximate the underlying system dynamics in a two-dimensional space. The topological signature is then approximated directly from geometric properties of this cloud rather than from persistence diagrams. Zero-dimensional features (H_0) are estimated from Euclidean distances between neighboring points, while one-dimensional features (H_1) are captured by fitting an ellipse to the point cloud and using the length of its minor axis as a surrogate for the persistence, or death time, of the dominant loop [11]. This ellipse-fitting step follows the direct least-squares formulation that guarantees an elliptical solution through a quadratic constraint on the conic parameters [12].

The present work builds on this Fast-TDA paradigm to develop a real-time, hardware-efficient shock-onset detection framework for high-rate electronic and PCB assemblies. Fast-TDA features are extracted from streaming acceleration measurements, the ellipse-fitting stage is implemented as a hardware-optimized pipeline on an FPGA using a cyclic Jacobi solver for the underlying generalized eigenvalue problem, and a sequential statistical test is applied to the resulting feature stream to localize shock onset with minimal latency. The framework is validated experimentally on a fixed-fixed beam platform subjected to controlled harmonic excitation followed by an imposed impulsive load. The aim of this study is to present a real-time shock-onset detection method for high-rate electronic systems by monitoring the changes in the geometric pattern of the fitted ellipse over datasets. When a shock is imposed on the system, the shape and orientation of the ellipse fitted to the delay-embedded point cloud change sharply. By tracking these rapid alterations in the ellipse pattern using Fast-TDA, the framework achieves deterministic low-latency detection while maintaining robustness to noise and non-stationarity. The paper code, data, and supporting artifacts are made available through a public repository to support reproducibility and reuse [13].

2. EXPERIMENTAL SETUP AND DATA ACQUISITION

The experimental setup, shown in Figure 1, consists of a fixed-fixed printed circuit board (PCB) assembly mounted on an electrodynamic shaker. A controlled voltage excitation signal is generated in LabVIEW and amplified by an LDS PA100E power amplifier before being supplied to the shaker. The shaker converts this electrical signal into mechanical vibration, which is applied to the PCB. The dynamic response of the board is measured using PCB Piezotronics 352A92 accelerometers mounted directly on the PCB. Acceleration signals are acquired at a sampling rate of 1 S/s through a NI cDAQ system interfaced with LabVIEW, enabling synchronized real-time recording of both the input excitation voltage and the output acceleration response.

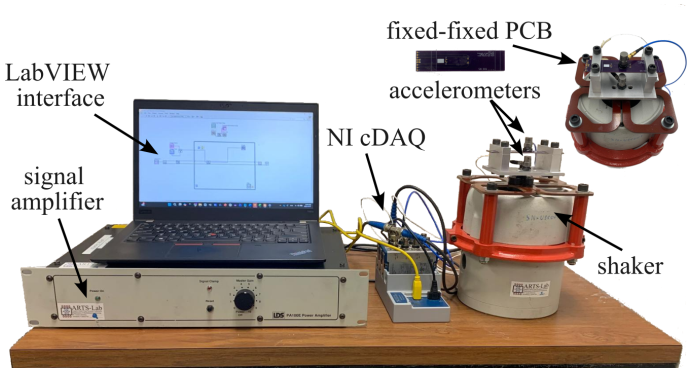

FIGURE 1: Experimental setup showing the fixed-fixed PCB assembly mounted on the shaker, together with the LabVIEW interface, signal amplifier, NI cDAQ, and accelerometers.

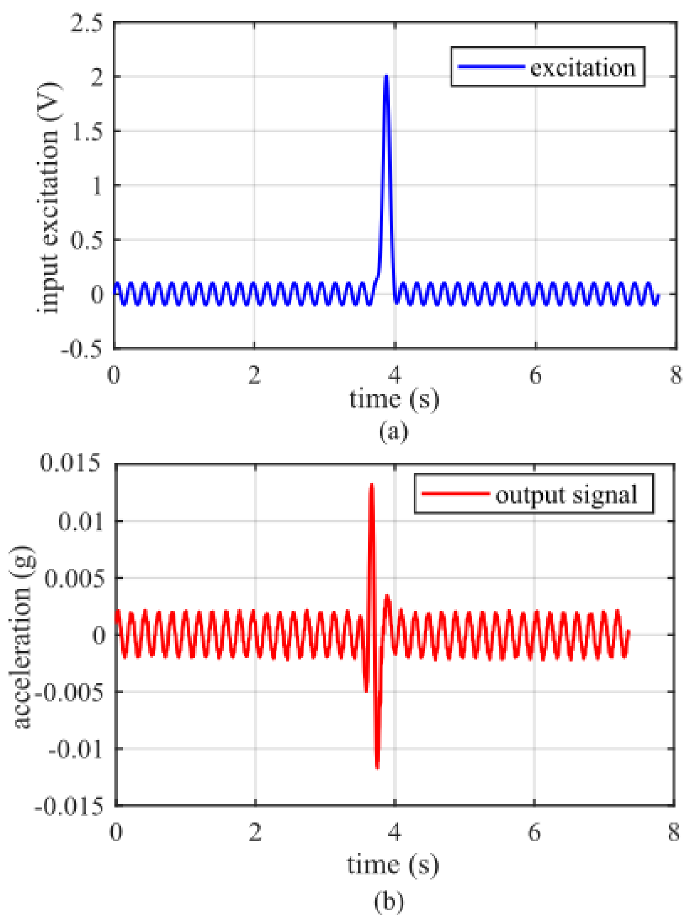

FIGURE 2: Time histories of the input excitation voltage applied to the shaker and the output acceleration response measured on the fixed-fixed PCB; showing: (a) input excitation voltage applied to the shaker; and (b) acceleration response measured on PCB.

The input excitation voltage applied to the shaker and the corresponding acceleration response measured on the PCB are shown in Figure 2. The input signal consists of a continuous low-amplitude harmonic excitation with a single impulsive shock superimposed at approximately 3.6 s. The output acceleration signal Figure 2(b), clearly captures the transient response induced by the shock. The acceleration trace clearly shows the steady-state harmonic vibration followed by a sharp transient spike at the instant the shock is applied, demonstrating the system's dynamic reaction to the sudden impulse.

These input-output signals constitute the raw high-rate time-series data used throughout this study. The sharp transient in the acceleration response at the shock instant produces a distinct change in the geometric pattern of the delay-embedded point cloud. This change is precisely what the proposed Fast-TDA method detects in real time by monitoring the minor-axis length of the fitted ellipse, thereby enabling low-latency shock-onset identification.

3. MATHEMATICAL DERIVATION

The general conic section is expressed as the algebraic implicit form:

$$F(\mathbf{x};\,\vec{a}) \;=\; ax^2 + bxy + cy^2 + dx + ey + f \;=\; 0 \tag{1}$$

where $\mathbf{x} = (x, y)^\top$ is a 2D data point, and $\vec{a} = [a, b, c, d, e, f]^\top \in \mathbb{R}^6$ is the vector of conic parameters. The parameters $[a, b, c]$ control the *shape* of the conic, while $[d, e, f]$ control its *position* and *scale*. For the conic to represent an ellipse, the following conditions must be met: discriminant condition must be satisfied:

$$b^2 - 4ac \;<\; 0 \tag{2}$$

Given N measured data points $\{(x_i,\, y_i)\}_{i=1}^{N}$, the design matrix $\mathbf{D} \in \mathbb{R}^{N\times 6}$ is constructed by expanding each point into the six conic basis terms: $\mathbf{D}[i,:] = [x_i^2,\; x_i y_i,\; y_i^2,\; x_i,\; y_i,\; 1]$. The 6×6 symmetric *scatter matrix* is then:

$$\mathbf{S} \;=\; \mathbf{D}^\top \mathbf{D} \tag{3}$$

$\mathbf{S}$ is always 6×6 regardless of N, making the downstream eigenvalue problem fixed in size and directly suitable for FPGA hardware implementation. The ellipse fitting problem seeks $\mathbf{a}$ that minimizes the sum of squared algebraic distances subject to the ellipse-enforcing constraint $4ac - b^2 = 1$:

$$\min_{\vec{a}} \;\; \vec{a}^\top \mathbf{S}\,\vec{a} \quad \text{subject to} \quad \vec{a}^\top \mathbf{C}\,\vec{a} \;=\; 1 \tag{4}$$

where $\mathbf{C} \in \mathbb{R}^{6\times 6}$ is the constraint matrix whose non-zero entries occupy only the upper-left 3×3 block $\mathbf{C}_{11}$, reflecting that only $[a, b, c]$ are constrained:

$$\mathbf{C}_{11} \;=\; \begin{bmatrix} 0 & 0 & 2 \\ 0 & -1 & 0 \\ 2 & 0 & 0 \end{bmatrix} \tag{5}$$

Applying Lagrange multipliers to Equation 4 yields the *generalized eigenvalue problem*:

$$\mathbf{S}\,\vec{a} \;=\; \lambda\,\mathbf{C}\,\vec{a} \tag{6}$$

where λ is the Lagrange multiplier (eigenvalue) and $\vec{a}$ is the corresponding eigenvector. The optimal ellipse corresponds to the eigenvector with the smallest positive eigenvalue $\lambda > 0$ that simultaneously satisfies the condition shown in Equation 2. Since the lower-right 3×3 block of $\mathbf{C}$ is zero, direct factorization fails on the full 6×6 system. Partitioning $\mathbf{S}$ into blocks according to $[a, b, c]$ (rows/cols 1–3) and $[d, e, f]$ (rows/cols 4–6), the unconstrained parameters $[d, e, f]$ are eliminated analytically via the *Schur complement*:

$$\widetilde{\mathbf{S}} \;=\; \mathbf{S}_{11} \;-\; \mathbf{S}_{12}\,\mathbf{S}_{22}^{-1}\,\mathbf{S}_{21} \tag{7}$$

where $\mathbf{S}_{11}$ captures interactions among $[a, b, c]$, $\mathbf{S}_{22}$ captures interactions among $[d, e, f]$, and $\mathbf{S}_{12} = \mathbf{S}_{21}^\top$ captures cross-interactions. $\widetilde{\mathbf{S}}$ is 3×3 and encodes the full scatter information with the influence of $[d, e, f]$ already absorbed. The constraint sub-matrix $\mathbf{C}_{11}$ is indefinite with zero diagonal entries, requiring a permuted LDL^T factorization with Bunch–Kaufman pivoting. A permutation $\mathbf{P}$ is determined such that:

$$\mathbf{P}\,\mathbf{C}_{11}\,\mathbf{P}^\top \;=\; \mathbf{L}_3\,\mathbf{D}_3\,\mathbf{L}_3^\top \tag{8}$$

where $\mathbf{L}_3$ is 3×3 lower triangular with unit diagonal, and $\mathbf{D}_3$ is block diagonal with non-zero determinant. The subscript 3 denotes the 3×3 reduced system. Using these factors, the reduced generalized eigenvalue problem is transformed into the *standard symmetric eigenvalue problem*:

$$\mathbf{A}\,\vec{z} \;=\; \lambda\,\vec{z}, \qquad \mathbf{A} \;=\; \mathbf{D}_3^{-1}\,\mathbf{L}_3^{-1}\,\widetilde{\mathbf{S}}_{\mathrm{p}}\,\mathbf{L}_3^{-\top} \tag{9}$$

where $\widetilde{\mathbf{S}}_{\mathrm{p}} = \mathbf{P}\widetilde{\mathbf{S}}\mathbf{P}^\top$ is the permuted Schur complement. $\mathbf{A}$ is 3×3 and symmetric, making it directly solvable by the cyclic Jacobi method on hardware.After solving Equation 9 via the cyclic Jacobi method, the shape parameters are recovered from the selected eigenvector $\vec{z}_k$ as: $\vec{a}_1^* = \mathbf{L}_3^{-\top}\vec{z}_k$ where k is the index of the smallest positive eigenvalue satisfying Equation 2. The position and scale parameters follow directly by matrix multiplication with no further eigenvalue computation:

$$\vec{a}^* \;=\; \begin{bmatrix} \vec{a}_1^* \\ \vec{a}_2^* \end{bmatrix} \;=\; \begin{bmatrix} \mathbf{L}_3^{-\top}\,\vec{z}_k \\ -\,\mathbf{S}_{22}^{-1}\,\mathbf{S}_{21}\,\vec{a}_1^* \end{bmatrix} \tag{10}$$

where $\vec{a}_1^* = [a, b, c]^\top$ defines the ellipse shape and $\vec{a}_2^* = [d, e, f]^\top$ defines its position and scale.

The ellipse fitting procedure is summarised in Algorithm 1. The scatter matrix $\mathbf{S}$ is first assembled from the N data points, then reduced from 6×6 to 3×3 via the Schur complement, which eliminates the unconstrained parameters $[d, e, f]$ analytically. The LDL$^\top$ factors $\mathbf{L}_3$, $\mathbf{D}_3$, and permutation $\mathbf{P}$, pre-computed offline from the fixed constraint matrix $\mathbf{C}_{11}$, are used to form the standard symmetric matrix $\mathbf{A}$. The cyclic Jacobi method then diagonalises $\mathbf{A}$, and the valid ellipse solution is identified by testing the eigenvalue sign and discriminant condition. The shape parameters $[a, b, c]$ are recovered from the selected eigenvector, and $[d, e, f]$ follow by a single matrix multiplication.

Algorithm 1 Direct Ellipse Fitting Pipeline

Require: N points $\{(x_i, y_i)\}_{i=1}^{N}$, threshold ε, offline constants $\mathbf{L}_3^{-1}$, $\mathbf{D}_3^{-1}$, $\mathbf{P}$

Ensure: $\vec{a}^* = [a, b, c, d, e, f]^\top$

// Stage 1: build scatter matrix

$\mathbf{D}[i, :] \leftarrow [x_i^2,\ x_i y_i,\ y_i^2,\ x_i,\ y_i,\ 1]$ — $\forall i$

$\mathbf{S} \leftarrow \mathbf{D}^\top \mathbf{D}$ — *always* 6×6

// Stage 2: partition S and Schur complement

$\mathbf{S}_{11} \leftarrow \mathbf{S}(1{:}3, 1{:}3),\ \mathbf{S}_{12} \leftarrow \mathbf{S}(1{:}3, 4{:}6),\ \mathbf{S}_{22} \leftarrow \mathbf{S}(4{:}6, 4{:}6)$

$\tilde{\mathbf{S}} \leftarrow \mathbf{S}_{11} - \mathbf{S}_{12}\mathbf{S}_{22}^{-1}\mathbf{S}_{21}$ — *reduced to* 3×3

// Stage 3: partition $\mathbf{C}_{11}$ *and form matrix* $\mathbf{A}$

$\mathbf{P}, \mathbf{L}_3, \mathbf{D}_3 \leftarrow \mathrm{ldl}(\mathbf{C}_{11})$ — *offline, hard-coded on FPGA*

$\mathbf{A} \leftarrow \mathbf{D}_3^{-1}\mathbf{L}_3^{-1}(\mathbf{P}\tilde{\mathbf{S}}\mathbf{P}^\top)\mathbf{L}_3^{-\top}$ — *symmetric,* 3×3

// Stage 4: cyclic Jacobi solver

$\mathbf{Z} \leftarrow \mathbf{I}_3$ — *initialise eigenvector matrix*

repeat

  $(p, q) \leftarrow \arg\max_{p<q} |A_{pq}|$ — *largest off-diagonal*

  $\tau \leftarrow (A_{qq} - A_{pp})/(2A_{pq})$

  $t \leftarrow \mathrm{sign}(\tau)/(|\tau| + \sqrt{1 + \tau^2})$

  $c \leftarrow 1/\sqrt{1 + t^2},\ s \leftarrow tc$ — *rotation in* (p, q) *plane*

  $\mathbf{A} \leftarrow \mathbf{J}^\top \mathbf{A}\mathbf{J},\ \mathbf{Z} \leftarrow \mathbf{Z}\mathbf{J}$ — *rows/cols* p, q *only*

until $\max_{p<q} |A_{pq}| < \varepsilon$ — *converged*

// Stage 5: select valid ellipse eigenvector

for $k = 1$ **to** 3 **do**

  $\vec{a}_1^{(k)} \leftarrow \mathbf{L}_3^{-\top}\vec{z}_k$ — $\vec{z}_k$ *= column* k *of* $\mathbf{Z}$

  if $\lambda_k > 0$ **and** $b^2 - 4ac < 0$ **then**

    $\vec{a}_1^{*(k)} \leftarrow \vec{a}_1^{(k)}$ — *smallest valid* λ_k

  end if

end for

// Stage 6: recover $\vec{a}_1^*$ *and* $\vec{a}_2^*$ *separately*

$\vec{a}_1^* = [a, b, c]^\top \leftarrow \mathbf{L}_3^{-\top}\vec{z}_{k^*}$ — *ellipse shape*

$\vec{a}_2^* = [d, e, f]^\top \leftarrow -\mathbf{S}_{22}^{-1}\mathbf{S}_{21}\vec{a}_1^*$ — *position and scale*

return $\vec{a}^* = [\vec{a}_1^{*\top},\ \vec{a}_2^{*\top}]^\top$ — *complete* $[a, b, c, d, e, f]^\top$

The LDL$^\top$ factors $\mathbf{L}_3^{-1}$, $\mathbf{D}_3^{-1}$, and $\mathbf{P}$ are computed once offline in MATLAB from the fixed constraint matrix $\mathbf{C}_{11}$ and hard-coded as constants in the Vitis HLS implementation, so no factorization is required at runtime. The only iterative component is the Jacobi loop in Stage 4, which converges in a small number of sweeps for a 3×3 symmetric matrix and relies solely on fixed plane rotations and localized two-row/two-column updates, making it well suited for pipelined FPGA execution with deterministic latency.

The pipeline is deliberately designed to minimize runtime complexity on FPGA hardware. By performing the Schur complement reduction in Stage 2, the problem size is reduced from a full 6×6 system to a compact 3×3 symmetric eigenproblem, eliminating the three unconstrained parameters analytically and avoiding unnecessary computation. The offline pre-computation of the LDL$^\top$ factors in Stage 3 further removes any matrix factorization from the real-time path, leaving only matrix multiplications and the cyclic Jacobi iterations. Because the Jacobi solver operates exclusively with simple rotations and local updates, the entire algorithm executes with fixed, deterministic latency that is independent of the input data, which is essential for reliable high-rate shock detection.

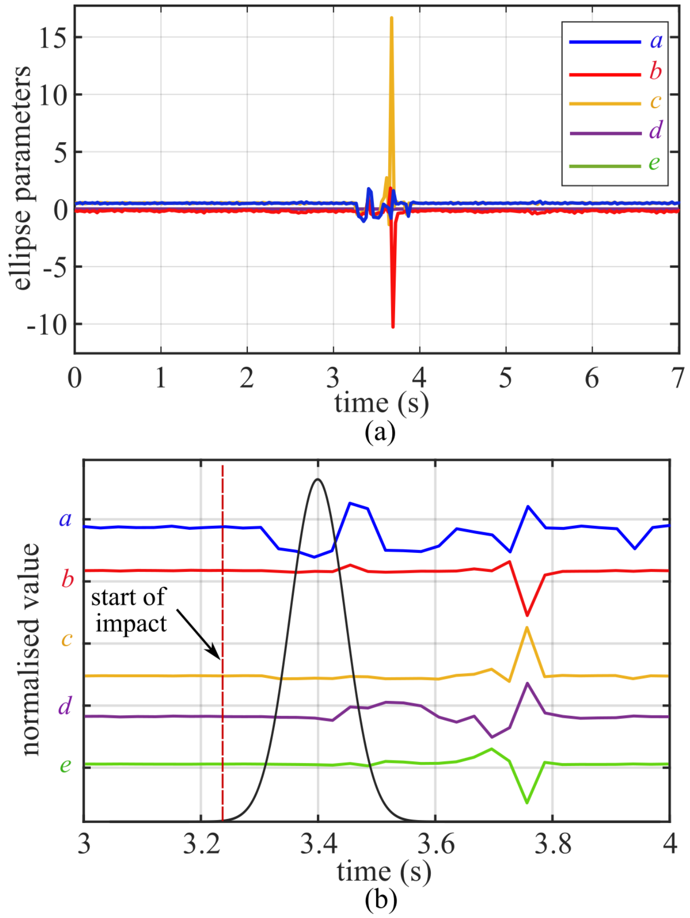

FIGURE 3: Evolution of the fitted ellipse parameters; showing: (a) raw coefficients; and (b) normalized values of the same coefficients along with the impact signal and red dashed line indicating the impact moment from the period of 3s to 4s showing the impact excitation signal in gray.

4. RESULTS AND DISCUSSION

The time evolution of the six ellipse parameters obtained from the Fast-TDA pipeline is shown in Figure 3(a). The parameters a, b, and c describe the quadratic form of the conic, namely, the shape and orientation of the ellipse, while d, e, and f control its position and scale. Prior to the shock event, which peaks at 3.4 s, all parameters remain nearly constant, reflecting the steady-state harmonic excitation of the system. At the instant of shock imposition, a sharp transient appears. Parameters b and c exhibit pronounced spikes, whereas d, e, and a show comparatively smaller deviations. These high spikes in the quadratic coefficients directly alter the shape of the orbit in the delay-embedded point cloud, demonstrating that the quadratic terms are highly responsive to sudden changes in the system dynamics.

To highlight sensitivity, the same coefficients are normalized using a min-max scaling procedure. For each parameter, the values are first shifted by their minimum and then divided by their range, with a safeguard that sets the range to unity when it falls below a small threshold to avoid division by zero. An additional vertical offset is applied to separate the traces for clear visualization. The normalized traces shown in The normalized

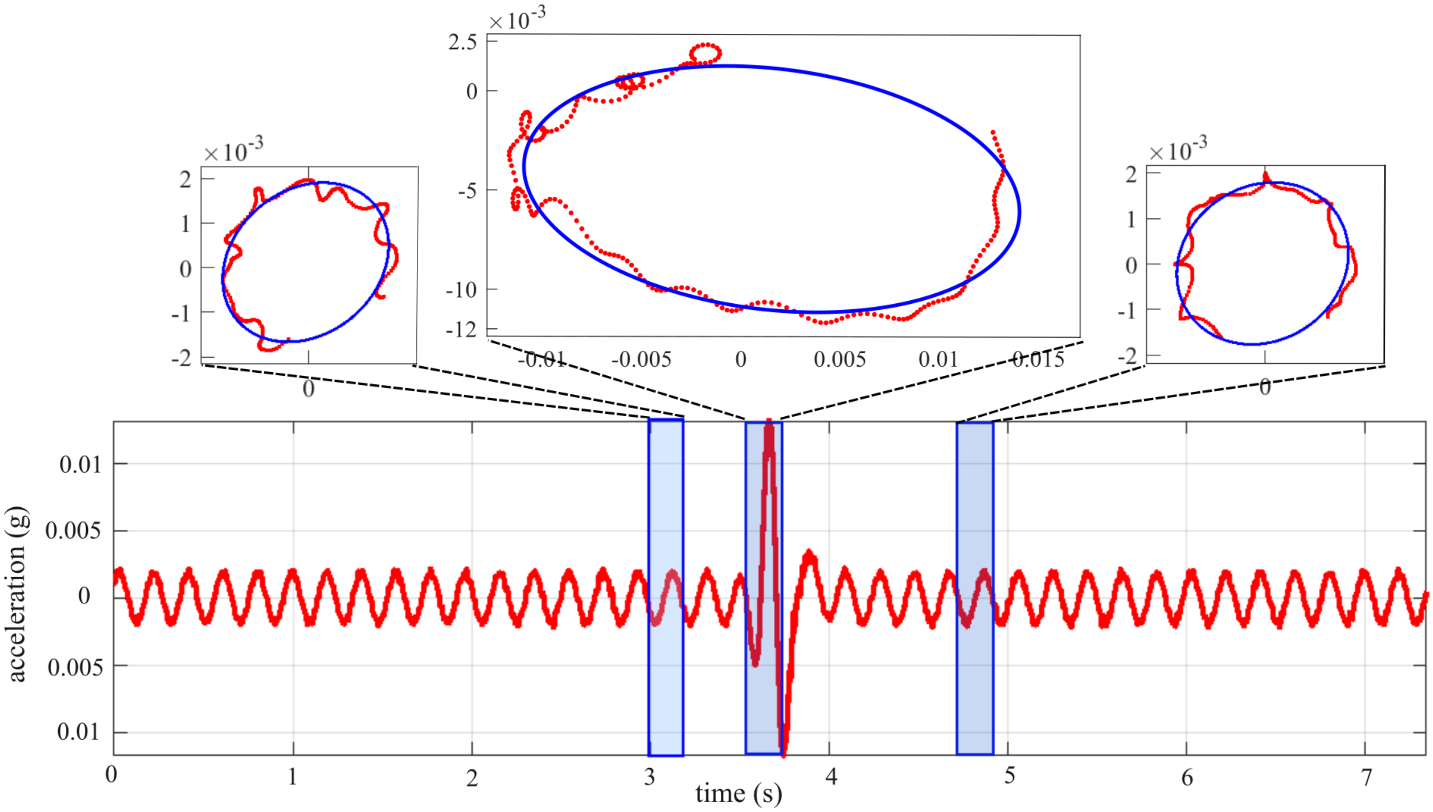

FIGURE 4: Acceleration response with sliding windows indicating three representative intervals: pre-shock steady vibration, shock event, and post-shock, which return to steady state; showing the display of the delay-embedded point cloud (blue) together with the fitted ellipse (red) at selected time instants.

traces shown in Figure 3(b) reveal that parameter a produces the fastest excursions immediately after the shock instant. In this subplot, the black peak represents the measured impact signal, and the red dashed line indicates the selected time at which the impact is imposed on the system. Prior to this moment, the normalized ellipse parameters remain nearly steady, reflecting the stable geometry of the delay-embedded point cloud under harmonic excitation.

The corresponding evolution of the actual ellipse geometry is visualized in Figure 4. The main panel shows the acceleration time series with shaded windows marking three representative intervals: pre-shock with steady vibration, shock onset as a transient moment, and post-shock, returning to steady state. Inset ellipses superimposed on the delay-embedded point clouds illustrate the geometric change. Before the shock, the cloud forms a tight, nearly circular orbit; during the shock, the ellipse elongates dramatically and rotates; after the shock, the ellipse returns to a compact shape sim ilar to the pre-shock condition. This visual evidence directly links the parameter transients observed in Figure 3 to measurable alterations in the point-cloud topology.

5. CONCLUSION

This study presented a real-time shock-onset detection framework for high-rate electronic and printed circuit board assemblies based on Fast-TDA, an approximate topological approach that extracts geometric surrogates from delay-embedded point clouds. By replacing the computationally intensive construction of persistence diagrams with direct ellipse fitting on two-dimensional point clouds, the method achieves a dramatic reduction in processing time while retaining the essential topological signature of sudden transients. The ellipse-fitting stage was implemented as a fully hardware-optimized pipeline on an FPGA using a cyclic Jacobi solver for the underlying generalized eigenvalue problem, delivering deterministic low-latency operation suitable for high sampling rates. Experimental validation on a fixed-fixed beam platform subjected to controlled harmonic excitation followed by an imposed impulsive load demonstrated that the quadratic coefficients, particularly parameter a, respond sharply to shock events and produce clear changes in the shape and orientation of the fitted ellipse. These geometric alterations were successfully captured by a sequential change-point detector, confirming that Fast-TDA can localize shock onset with minimal delay and high robustness to steady-state vibration.

The proposed approach offers two primary advantages over conventional full TDA pipelines. First, it eliminates the need for persistence diagram computation at every time window, thereby enabling real-time execution on resource-constrained embedded hardware. Second, the ellipse parameters themselves serve as physically interpret able monitoring features that directly reflect changes in the underlying system dynamics. The framework, therefore, provides both low-latency detection performance and a transparent geometric interpretation of the detected events. These attributes make Fast-TDA particularly well-suited for safety-critical applications in high-rate environments where rapid and reliable shock identification is essential.

Future work will focus on the complete hardware implementation of the Fast-TDA algorithm on an FPGA using High-Level Synthesis (HLS). This development will include integration of the change-point detection logic on the same FPGA, further optimization for higher sampling rates, and extensive experimental validation on additional high-rate platforms. Overall, the results demonstrate that approximate topological analysis combined with efficient FPGA implementation constitutes a promising pathway toward practical, real-time structural health monitoring in high-rate dynamic systems.

ACKNOWLEDGMENTS

This material is based upon work supported by the National Science Foundation grant numbers CCF - 1956071, CCF-2234921, and CPS - 2237696. Any opinions, findings conclusions, or recommendations expressed in this material are those of the authors and do not necessarily reflect the views of the National Science Foundation.

REFERENCES

[1] Dodson, Jacob, Downey, Austin, Laflamme, Simon, Todd, Michael D., Moura, Adriane G., Wang, Yang, Mao, Zhu, Avitabile, Peter and Blasch, Erik. *High-Rate Structural Health Monitoring and Prognostics: An Overview*. Springer International Publishing (2021): pp. 213–217. DOI 10.1007/978-3-030-76004-5_23.

[2] Razmarashooli, Arman, Chua, Yang Kang, Barzegar, Vahid, Salazar, Daniel, Laflamme, Simon, Hu, Chao, Downey, Austin R.J., Dodson, Jacob and Schrader, Paul T. "Real-time state estimation of nonstationary systems through dominant fundamental frequency using topological data analysis features." *Mechanical Systems and Signal Processing* Vol. 224 (2025): p. 112048. DOI 10.1016/j.ymssp.2024.112048.

[3] Zhou, Zhidai, Chen, Jiahuan, Yu, Chen, Wang, Yuxin and Zhang, Yu. "Failure Analysis of Printed Circuit Board Solder Joint under Thermal Shock." *Coatings* Vol. 13 No. 3 (2023): p. 572. DOI 10.3390/coatings13030572.

[4] Luan, Jing-en, Tee, Tong Yan, Pek, Eric, Lim, Chwee Teck and Zhong, Zhaowei. "Dynamic responses and solder joint reliability under board level drop test." *Microelectronics Reliability* Vol. 47 No. 2-3 (2007): pp. 450–460. DOI 10.1016/j.microrel.2006.05.012.

[5] Tanweer, Sunia, A. Khasawneh, Firas, Munch, Elizabeth and R. Tempelman, Joshua. "A topological framework for identifying phenomenological bifurcations in stochastic dynamical systems." *Nonlinear Dynamics* Vol. 112 No. 6 (2024): pp. 4687–4703. DOI 10.1007/s11071-024-09289-1.

[6] Esser, B. and Huston, D. "Active mass damping of electronic circuit boards." *Journal of Sound and Vibration* Vol. 277 No. 1-2 (2004): pp. 419–428. DOI 10.1016/j.jsv.2003.11.055.

[7] Wu, Zhiwei. "Active vibration control of rotating smart bidirectional FGPTC subjected to internal mechanical shock." *Mechanics Based Design of Structures and Machines* Vol. 52 No. 11 (2024): pp. 9015–9036. DOI 10.1080/15397734.2024.2335203.

[8] Roberts, Trotter, Gol Zardian, Mohsen, Satme, Joud N. and Downey, Austin R. J. "Finite Element Modeling of Fixed-Fixed Beams Under Shock Excitation With Active Control." *Volume 5: Dynamics, Vibration, and Control*. 2025. American Society of Mechanical Engineers. DOI 10.1115/imece2025-166672.

[9] Tempelman, Joshua R. and Khasawneh, Firas A. "A look into chaos detection through topological data analysis." *Physica D: Nonlinear Phenomena* Vol. 406 (2020): p. 132446. DOI 10.1016/j.physd.2020.132446.

[10] Gowdridge, T., Dervilis, N. and Worden, K. "On Topological Data Analysis for Structural Dynamics: An Introduction to Persistent Homology." *ASME Open Journal of Engineering* Vol. 1 (2022). DOI 10.1115/1.4055184.

[11] Salazar Martinez, Daniel A., Razmarashooli, Arman, Chua, Yang Kang, Laflamme, Simon, Hu, Chao, Schrader, Paul T., Downey, Austin R. J., Bakos, Jason D., Begashaw, Negash, Comert, Gurcan and Dodson, Jacob. *Fast Topological Data Analysis Features for Nonstationary Time Series*. Springer Nature Switzerland (2025): pp. 364–371. DOI 10.1007/978-3-031-94895-4_38.

[12] Fitzgibbon, A., Pilu, M. and Fisher, R.B. "Direct least square fitting of ellipses." *IEEE Transactions on Pattern Analysis and Machine Intelligence* Vol. 21 No. 5 (1999): pp. 476–480. DOI 10.1109/34.765658.

[13] Mohsen Gol Zardian, Austin R. J. Downey Jason D. Bakos, Charlton Rolle. "Paper 2026 FPGA-deployable Approximate Topological Framework." GitHub (2026). URL https://github.com/ARTS-Laboratory/Paper-2026-FPGA-deployable-Approximate-Topological-Framework.